

THE PHYSICS OF NUCLEUS - NUCLEUS FUSION AND SYNTHESIS OF SUPER HEAVY NUCLEI

Władysław J. Świątecki
Nuclear Science Division
Lawrence Berkeley National Laboratory
Berkeley, California 94720, USA
e-mail: WJSwiatecki@lbl.gov

Krystyna Siwek-Wilczyńska
Institute of Experimental Physics
University of Warsaw
Hoża 69, 00-681 Warsaw, Poland
e-mail: siwek@fuw.edu.pl

Janusz Wilczyński
Andrzej Sołtan Institute for Nuclear Studies
05-400 Otwock-Świerk, Poland
e-mail: wilczynski@ipj.gov.pl

(Received 10 June 2008; accepted 15 June 2008)

Abstract

A descriptive account is given of the “Fusion by Diffusion” theory of nucleus-nucleus amalgamation. The stress is on explaining the physical elements that go into a theory that provides a general conceptual framework for describing nucleus-nucleus fusion, but whose detailed implementation is subject to some flexibility. Despite notable successes, the theory is in need of improvements both as regards the inclusion of important physical refinements and the optimal choice of its adjustable parameter(s).

1 Introduction

The topic of this article is how to make a very heavy nucleus out of two lighter ones. In the last 40-50 years we have learned a lot about this problem from experiments carried out at many nuclear physics laboratories in the world (see review articles of Hofmann [1] and Oganessian [2]), but understanding the physics of fusion of very heavy nuclear systems is still a central topic of research in nuclear physics. This article will focus on the approach to this problem formulated in Refs. [3, 4, 5] and known as the Fusion by Diffusion Model that we have been developing in the past few years. We will not attempt to review other theories in this field, some of them based on closely related physics. Compared to those theories, our description is weighted towards simplicity and algebraic rather than computer-intensive techniques. Progressively more comprehensive comparisons with experimental data will determine the degree of usefulness of such a simplified approach.

2 Experimental data

Broadly speaking there are two types of experiments aiming to produce very heavy nuclei in the range of atomic numbers $Z = 102$ to $Z = 118$: the hot and cold fusion reactions. The former uses the neutron rich projectile ^{48}Ca to bombard targets such as U, Pu, Am, Cm and Cf. The latter uses targets of ^{208}Pb or ^{209}Bi and projectiles ranging from Ca to Kr (see Fig. 1). In the hot fusion reactions the excitation energy of the resulting compound nucleus is such that typically at least three neutrons have to be evaporated to cool down the

The physics of nucleus-nucleus fusion and synthesis of super heavy nuclei

nucleus to its ground state. In cold fusion reactions only one neutron needs to be evaporated as a rule. This makes it considerably easier to estimate theoretically the relevant cross sections and we will focus on the cold fusion reactions as the best candidates for disentangling the physics of what goes on in nucleus-nucleus amalgamation.

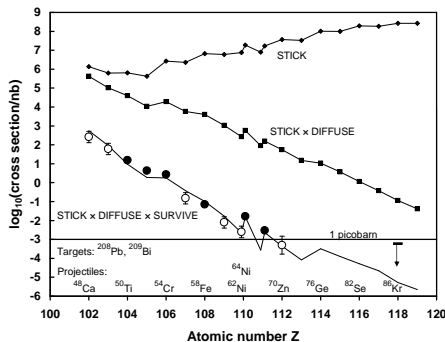


Figure 1: This is a comparison of the logarithms of theoretical and experimental peak cross sections for making elements with atomic numbers from 102 to 118 in one-neutron-out reactions using targets of ^{208}Pb and ^{209}Bi bombarded with the projectiles listed along the Z -axis. The solid circles refer to measured peak values, the open circles to estimates based on the values measured only at one or two energies. The uppermost curve shows the calculated cross sections for overcoming the Coulomb barrier, the middle curve the cross sections for forming a compound nucleus. See text. Figure taken from [3].

At this time there exist some 18 measurements providing information (sometimes very fragmentary) on the excitation functions for producing evaporation residues in cold fusion reactions. The cross sections range from about 300 nb for $Z = 102$ to about 0.00005 nb for $Z = 113$ [6]. Plotted on a logarithmic scale one sees a roughly

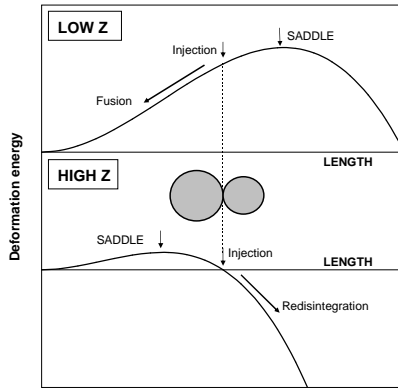


Figure 2: Schematic explanation of the appearance of a hindrance to fusion for very heavy nuclear systems. For light reacting systems the tangent configuration is on the inside of the saddle point shape in elongation space. Beyond a critical size of the reacting system the saddle moves inside the tangent configuration and an uphill diffusion is necessary for the system to reach the compound nucleus configuration. Figure taken from [3].

linear trend with Z showing a total decrease of 6.5 orders of magnitude, or an average factor of about 4 per one increment in Z (see Fig. 1). The striking feature of this trend is the implication that some new physics has entered the mechanism of fusion for reactions between heavy target-projectile combinations, those where the product of the two atomic numbers exceeds about 1600. This is because conventional theories that work well for reactions between lighter nuclei, when applied to the heavier ones, overestimate the cross sections by factors that reach almost six orders of magnitude in the case of $Z = 112$. These conventional theories consider the cross section for amalgamating two lighter nuclei into a heavier one in its ground state as the product of two factors: the cross section for the target and projectile to stick, and the probability for the excited compound nucleus

The physics of nucleus-nucleus fusion and synthesis of super heavy nuclei

(assumed to be formed automatically after sticking) to survive fission (as well as the emission of a second neutron if the cross section in question refers to a one-neutron-out reaction). Thus:

$$\text{Fusion} = \text{Stick} \times \text{Survive}. \quad (1)$$

The abovementioned data suggest that for the heavier reactions there appears a third factor, a hindrance to fusion (see Fig. 1). So the first challenge is to understand the reason for this "fusion hindrance" for reactions between very heavy nuclei.

3 The fusion hindrance

The qualitative reason for the hindrance has, in fact, been known since the eighties and has to do with a simple geometrical feature [7]. One needs to recall that a nucleus owes its stability to the existence of a local minimum or hollow in the (multidimensional) deformation space describing the nuclear potential energy considered as a function of the relevant disintegration degrees of freedom. The least energy required for a nucleus to climb out of the hollow is the energy of a "saddle point pass" in the mountain range surrounding the hollow. (There is usually more than one distinct saddle point pass present.) In the case of disintegration using shape degrees of freedom, this is the saddle point for fission. Conversely, in order for the configuration of two approaching nuclei to enter the compound nucleus hollow, the fusing system must find its way from the configuration of tangent target and projectile to the inside of the fission saddle point. The chance of doing this will depend strongly on whether the compactness (say the overall tip to tip length) of the tangent configuration is smaller or greater than the compactness of the saddle point. For light systems the saddle point shape is known to be a fairly elongated dumb-bell like configuration, longer than a typical configuration of two heavy nuclei in contact. In such cases fusion may be expected to take place automatically after contact. But, as is well known, with increasing fissility (roughly proportional to Z^2/A) the saddle point configuration begins to change from the dumb-bell shape towards the spherical configuration (sometimes modified somewhat by shell effects). This implies that at some critical size of the reacting system

(a critical fissility) the tangent configuration will find itself *on the outside* of the saddle and, after contact, the system will no longer amalgamate automatically into a compound nucleus (see Fig. 2). The reaction will experience a fusion hindrance caused by the need for the system to climb uphill over the saddle, starting from the “wrong side of the barrier”. The greater the excess of the fissility over the critical value, the more compact the saddle shape and the greater the hindrance to fusion. So, qualitatively, the existence of a fusion hindrance is a question of geometry, the relative compactness of the tangent and saddle configurations.

4 Diffusion over the fission barrier

In a deterministic dynamical process, if the starting (injection) point is on the wrong side of a (fission) barrier, the system will disintegrate with 100% probability. The probability to fuse will be zero. Disregarding quantal barrier penetration, the only chance for the system to fuse will be to rely on thermal fluctuations in the (shape) degrees of freedom. (One could increase the bombarding energy in order to brute-force the system into the hollow, but the price paid in the attending increase in compound nucleus excitation makes this impractical, at least for cold fusion reactions.) On the other hand a thermal fluctuation in the compactness can occasionally carry the system over the barrier into the compound nucleus hollow without increasing the excitation. Idealizing this process as a one-dimensional diffusion over a parabolic barrier (akin to a Brownian diffusion of a particle suspended in a viscous fluid at temperature T and in the presence of a linear field of force) one readily looks up in a textbook [8] the probability $P(\text{diffuse})$ that a system started off on the outside of a barrier at an energy H below its top will achieve fusion, viz.

$$P(\text{diffuse}) = \frac{1}{2}(1 - \text{erf}\sqrt{H/T}). \quad (2)$$

This becomes approximately proportional to a familiar Boltzmann factor $\exp(-H/T)$ soon after the argument of the error function has exceeded 1. As an approximation to the effective constant temperature which, in the nuclear case, is not constant but decreases from an initial temperature $T(\text{injection})$ to a lower temperature $T(\text{saddle})$

at the top of the barrier, we originally used the former, but later changed to the more reasonable geometrical mean between the two.

5 The “neck zip”

In order to estimate the Boltzmann argument H/T we make use of an anticipated separation of time scales in the post contact dynamics of target and projectile. It is an everyday observation that contact of two macroscopic drops initiates a very rapid growth of the neck connecting the two pieces, a “neck zip” much faster than the characteristic speeds of other collective degrees of freedom, such as the overall length or the mass ratio of the two pieces. This phenomenon is readily observed in the case of the fusion of two drops/discs of oil floating on water. The fusing of grease circles on the surface of chicken broth provides a familiar example. (An even simpler demonstration of the zip consists of wetting one’s thumb and forefinger and slowly bringing them together. At the instant that the two juxtaposed liquid surfaces touch, a zip takes place, creating a spindle-like liquid neck between the fingers.) The rapidity of the neck zip is due to the large saving in surface energy associated with the filling in of the crevice between the surfaces of the touching drops. The large driving force due to the saving in surface energy is resisted by inertial and/or dissipative forces, but these forces are necessarily small, because they are associated with the rearrangement of only small amounts of matter needed to fill in the crevice. This macroscopic argument appears to be sufficiently general so that it might have a fair degree of relevance also in the nuclear context but, because of the diffuseness of nuclear surfaces, the zip may not be as rapid relative to the other degrees of freedom as for sharp-surfaced drops.

Accepting this separation of time scales, one expects that after contact the neck will grow rapidly at an approximately fixed asymmetry and elongation (compactness) of the system. The growth is expected to carry the system towards the bottom of an “asymmetric fission valley”. This we define as the configuration that minimizes the potential energy with respect to the neck degree of freedom at fixed asymmetry and overall elongation. (Recall the spindle-like neck between the wetted thumb and forefinger.) Since immediately after contact the temperature of the system is close to zero, thermal diffusion will tend to be weighted towards the vicinity of the asymmetric

fission valley, where the temperature is highest. In addition, owing to the initial speed of the zip, little time is available for thermal diffusion in the early stages of the neck growth. An extreme idealization would thus be to assume that the “injection point” at which diffusion effectively begins, is at the bottom of the asymmetric fission valley. The crudeness of this assumption may be mitigated by the introduction at this stage of an adjustable parameter, namely the effective separation between the nuclear surfaces where the neck zip is assumed to take place. Formally, the zip is associated with a loss of stability in the neck-growth degree of freedom. For drops with sharp surfaces this loss of stability takes place at the instant of touching. In the nuclear case the surfaces have considerable diffuseness, of the order of 3 fm. We have not so far succeeded to estimate from first principles at what separation of the diffuse surfaces a zip should take place. (In order of magnitude the distance should be related to the range of nuclear forces.) We shall consider this distance, s , as specified by (say) the separation between the “equivalent sharp” nuclear surfaces, to be an adjustable parameter of our theory. We would expect s to be somewhere in the range between 0 and 3 fm.

6 The deformation energy along the asymmetric fission valley

In order to estimate this energy we use the familiar parameterization of nuclear shapes by two (unequal) spheres joined smoothly by a third quadratic surface of revolution in the form of a piece of a spheroid, a cone or a hyperboloid of one or two sheets. The macroscopic (liquid drop) energies of such configurations had been tabulated some time ago as functions of three degrees of freedom: elongation, asymmetry and neck size [9]. By fitting simple polynomials to the tabulated values in the relevant range of deformations, it is possible to minimize explicitly the energy with respect to neck size at fixed asymmetry and elongation. There results an algebraic expression for the (macroscopic) deformation energy along the asymmetric fission valley (see Ref. [3], Appendix A). This deformation energy is then plotted as a function of the overall tip-to-tip elongation of the system or, equivalently, as a function of that elongation decreased by the sum of the diameters of the colliding nuclei, as shown in Fig. 3.

The physics of nucleus-nucleus fusion and synthesis of super heavy nuclei

The reason for the latter choice of variable is that, in the entrance channel, this quantity is just the separation, s , between the surfaces of the approaching nuclei. According to the abovementioned idealization one expects the thermal diffusion in the asymmetric fission valley to begin at a value of s in the range between about 0 and 3 fm.

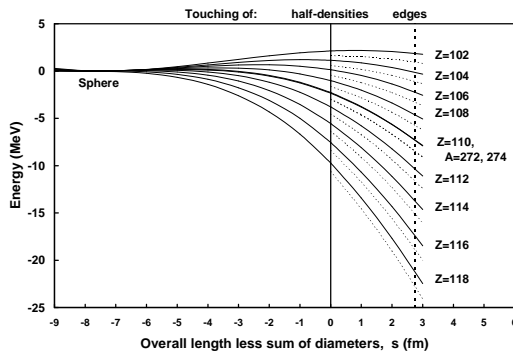


Figure 3: The macroscopic deformation energies along the asymmetric fission valley for 20 reactions ranging from $^{48}\text{Ca} + ^{208}\text{Pb}$ to $^{86}\text{Kr} + ^{209}\text{Bi}$, as functions of s , equal to the excess of the length of the configuration over the sum of the target and projectile diameters. In the entrance channel of two approaching nuclei a length specified by $s = 0$ would correspond to contact of the half-density contours, and $s \approx 2.74$ fm to the contact between the classical turning points for the nucleons at the Fermi energy. Figure taken from [3].

A glance at the resulting deformation energies along the asymmetric fission valleys for the cold fusion systems with $Z = 102$ to $Z = 118$ reveals the following situation illustrated in Fig. 3. In the range $0 < s < 3$ fm the deformation energy is virtually flat in the case of $Z = 102$, indicating no need for an uphill diffusion to enter

the compound nucleus hollow. Thus no hindrance to fusion. On the other hand, in the above range of s , a considerable hindrance would be expected for $Z = 112$. The injection point lies between 4 and 10 MeV below the level of the saddle-point energy in this case - see Sec.12. For $Z = 118$ the estimated injection energies in the range $0 < s < 3$ fm would be somewhere between 10 and 21 MeV below the saddle energy.

7 An estimate of the hindrance

As mentioned above, the injection separation s will be treated as an adjustable parameter. Once this is chosen, an estimate of the potential energy at injection is available. In order to estimate H , the height of the barrier to be overcome by diffusion, one also needs an estimate of the energy of the relevant saddle point for fission. In the cases of interest the mass of the fission saddle point turns out to be roughly equal to the mass of the macroscopic spherical configuration, as shown in Sec. 12. The other term in the Boltzmann argument H/T is the effective temperature T , which we take to be the geometric mean between $T(\text{injection})$ and $T(\text{saddle})$. These temperatures are estimated from the nuclear excitations at injection and at saddle, equal to the differences between the center of mass energy for the reaction in question and the potential energies of the injection point and of the saddle, respectively. For all the cold fusion reactions in question T turns out to be close to 0.6 MeV.

Taking the observed hindrance in the case of $Z = 112$ as about 10^{-6} , and applying Eq. (2), we find $H/T \approx 11.3$ and $H \approx 6.8$ MeV. This is in the range of hindrance barriers for $Z = 112$ that we estimated above. It turns out to correspond to an injection separation s of about 1.4 fm (see Fig.3). Thus we seem to be on the right track and can go on to combine the hindrance factor which we shall call “Diffuse” with the other two (conventional) factors and write the cross section for fusion as

$$\text{Fusion} = \text{Stick} \times \text{Diffuse} \times \text{Survive}. \quad (3)$$

8 Cross section for sticking

This is the cross section for the target and projectile to come into sufficiently intimate contact, so that immediate re-separation

is avoided and, instead of two sub-systems, one is dealing with a single “composite” nucleus. This cross section is often identified with the cross section to overcome a “Coulomb barrier,” the maximum in the potential energy of target and projectile plotted as a function of some suitable approach degree of freedom. In view of our discussion of the neck zip, it is necessary to modify this concept of sticking. For systems with diffuse surfaces it may well happen that a neck zip takes place at a separation between the surfaces which is larger than the location of the Coulomb barrier. Since a neck zip certainly ensures the formation of a stuck, composite mononucleus, the more nearly correct way of defining the criterion for sticking is in terms of a loss of equilibrium in the neck-growth degree of freedom at a critical value of the approach degree of freedom. (R. Bass recognized clearly in 1974 the need to distinguish between a Coulomb barrier and an “interaction barrier,” analogous to our sticking barrier [10].)

The formula for the sticking cross section that we use was patterned on the “barrier distribution scheme” in which one starts with the familiar classical formula for the cross section to overcome a barrier B encountered at separation R between two mass points colliding with center of mass energy E , viz. $\pi R^2(1 - B/E)$. This formula is then generalized by imagining that one is dealing with an assembly of collisions characterized by a Gaussian distribution of barriers around a mean B_0 , with the result:

$$\text{Stick} = \pi R^2 \frac{v}{2E} \left[X(1 + \operatorname{erf} X) + \frac{1}{\sqrt{\pi}} \exp(-X^2) \right], \quad (4)$$

where $X = (E - B_0)/v$, and v is the range of the Gaussian.

For $E \gg B_0$ the resulting cross section approaches the geometrical limit πR^2 . For $E < B_0$ it decreases more and more rapidly, eventually at a precipitous rate proportional to $\exp[-(E - B_0)^2/v^2]$, and thus *even faster than an exponential*. This feature has an interesting effect on the predicted shape of the fusion excitation function, as discussed in Sec. 14. Note that Eq. (4) holds independently of whether B is considered to be the Coulomb barrier or, more correctly, the sticking barrier.

In Figs. 4 and 5 we give several examples how well Eq. (4) fits fusion excitation functions for not too heavy nuclear systems, for

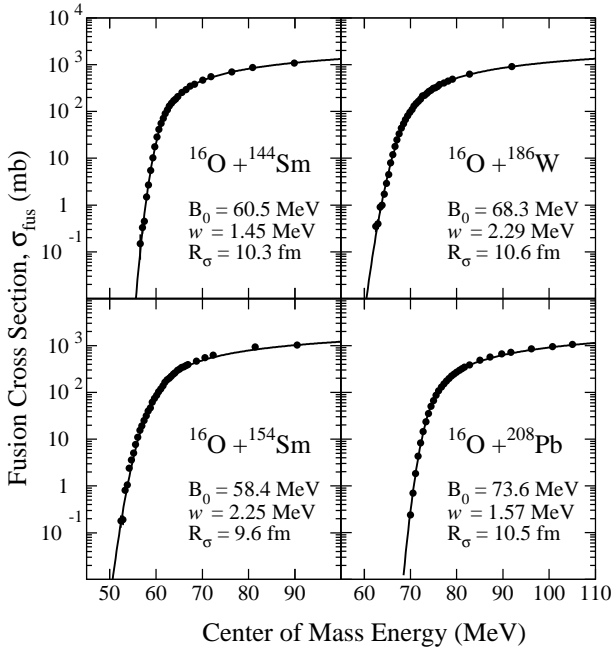


Figure 4: Fusion excitation functions measured for the $^{16}\text{O} + ^{144,154}\text{Sm}$ [12], $^{16}\text{O} + ^{186}\text{W}$, and $^{16}\text{O} + ^{208}\text{Pb}$ [13] reactions (full circles) compared with predictions (solid lines) of the “diffused barrier formula”, Eq. (4), for values of B_0 , w and R_σ obtained with the least-square method. In notation of Eq. (4) $w = v/\sqrt{2}$ and $R_\sigma = R$. Figure taken from [11].

which the overcoming the Coulomb barrier inevitably leads to fusion. In Ref. [11] a set of over 50 reactions, for which data on precisely measured fusion excitation functions are available in the literature, had been analyzed in terms of Eq. (4) and thus parameters needed to use this equation for predicting the sticking cross sections had been determined.

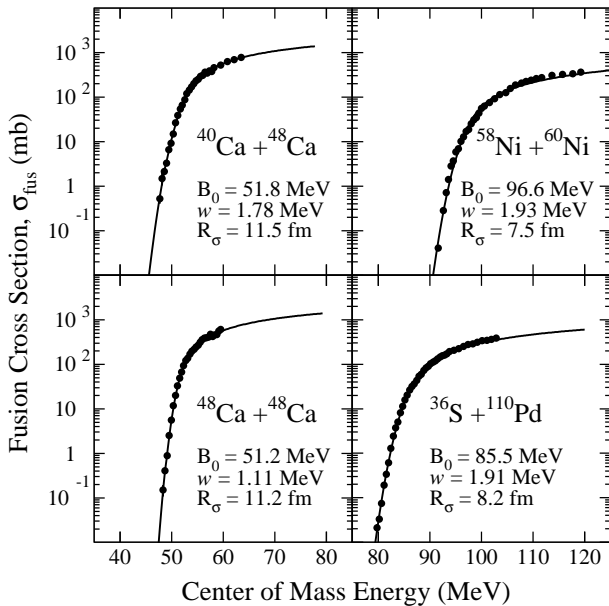


Figure 5: Fusion excitation functions measured for the $^{48}\text{Ca} + ^{40,48}\text{Ca}$ [14], $^{58}\text{Ni} + ^{60}\text{Ni}$ [15], and $^{36}\text{S} + ^{110}\text{Pd}$ [16] reactions (full circles) compared with predictions (solid lines) of the “diffused barrier formula”, Eq. (4), for values of B_0 , w and R_σ obtained with the least-square method. In notation of Eq. (4) $w = v/\sqrt{2}$ and $R_\sigma = R$. Figure taken from [11].

9 Survival probability: competition between neutron emission and fission

We use conventional transition state theory to estimate the relative probability for the disintegration of the excited compound nucleus by neutron emission or fission. This theory predicts this ratio to be the ratio N_n/N_f of the number of levels (decay “channels”) available to the system at the corresponding saddle point configurations. For neutron emission the saddle point is the configuration of the residual nucleus with a neutron (just) outside its surface. For fission it is the fission saddle point configuration. The number of levels in question is the number of excited states in the slots between

the energy (or mass) of the colliding system, including its center of mass energy, and the masses of the respective saddle points. Note that it is in the nature of things that the ratio N_n/N_f does not require the knowledge of any property of the compound nucleus, such as its neutron separation energy or its fission barrier. In view of a prevalent misconception regarding this point, we would like to stress that, in particular, N_n/N_f does not care about any dependence of the height of the fission barrier on excitation due to a washing out of a shell correction in the ground state of the compound nucleus. What one does need in order to estimate N_n/N_f for a given center of mass energy are the masses of the two saddle points and expressions for their level densities when in an excited state (see Fig. 6).

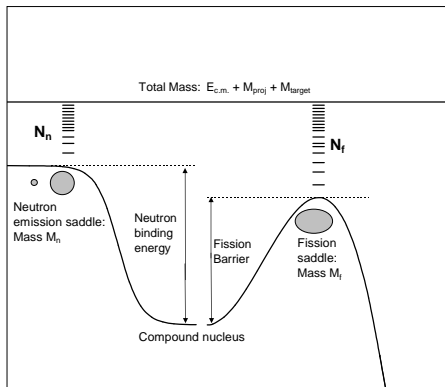


Figure 6: The relative decay probability by neutron emission or fission is the ratio N_n/N_f of the number of levels (“channels”) in the energy intervals between the total available energy (or mass in energy units) and the masses of the neutron emission or fission saddle points, M_n or M_f , respectively. Figure taken from [3]

10 Survival probability: avoiding second chance fission

Even after the excited compound nucleus has managed to avoid fission by emitting a neutron in the first round of the competition between the two modes of decay, it might still have sufficient excitation to either emit a second neutron or to fission (depending on which of the two decay modes has a lower threshold). In all the cold fusion reactions in question the fission threshold is lower, so in what follows we will refer to the avoidance of second chance fission, but the same formalism applies if the second neutron threshold is lower. (Recall that we have confined our discussion to one-neutron-out reactions, so emitting a second neutron must also be avoided.) If the center of mass energy E exceeds the second chance fission threshold E_{th} , say, the way to nevertheless avoid fission is to arrange for the (first) emitted neutron to have been evaporated with sufficient kinetic energy to bring back the available energy below the threshold value. This probability, $P(K)$, is an integral from $K \equiv E - E_{th}$ to infinity over the neutron's evaporation spectrum. Using a standard expression for this spectrum one finds [3]

$$P(K) = \left(1 + \frac{K}{T}\right) \exp\left(-\frac{K}{T}\right) \quad \text{for } K > 0, \quad (5)$$

where T is the temperature of the residual nucleus, typically about 0.6 MeV in our case. When $K < 0$, i.e. when E does not exceed E_{th} , $P(K) = 1$. This function $P(K)$ provides a very sharp cut off, with a width of about 0.6 MeV, for the otherwise steeply increasing cross section (see Sec. 13). The factor "Survive" in Eq. (3) is the product of N_n/N_f and $P(K)$.

As mentioned above, in reactions at higher excitation energies more neutrons than just one are emitted. Therefore the notion "Survive" means then that a final compound-residue nucleus reaches its ground state avoiding fission all the way of the multi-step deexcitation cascade of light particle emission. Calculation of the survival probability in such a general case of "hot fusion" reaction is a complex multi-branch problem that can be solved only with the Monte Carlo method. A detailed description of the fission-evaporation competition at higher excitation energies is given in Ref. [17] and compar-

isons of the calculated survival probabilities with experimental data are shown in Figs. 7 and 8.

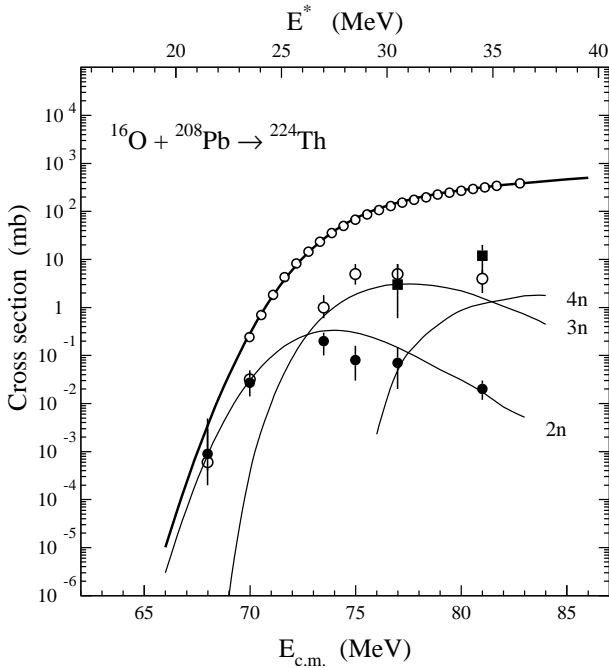


Figure 7: Evaporation residue cross sections for 2n, 3n and 4n reaction channels (full circles, open circles, and full squares, respectively) in the $^{16}\text{O} + ^{208}\text{Pb}$ reaction [18] and measured fusion excitation function for this reaction (small open circles) [19]. Theoretical predictions [17] (solid lines) represent the product of the sticking cross section given by Eq. (4) (thick solid line) and survival probability calculated with the Monte Carlo method. Figure taken from [17].

11 The level densities

For the level densities entering N_n/N_f we use the formula for a degenerate Fermi gas modified by conventional corrections for shell

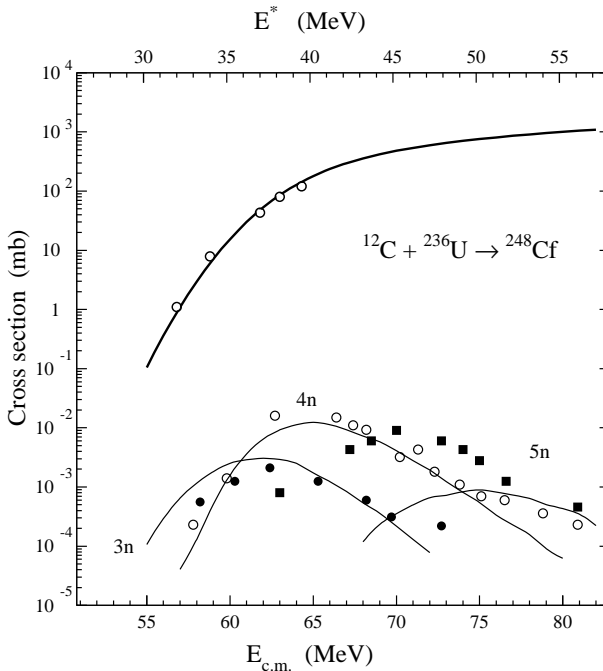


Figure 8: Evaporation residue cross sections for 3n, 4n and 5n reaction channels (full circles, open circles, and full squares, respectively) in the $^{12}\text{C} + ^{236}\text{U}$ reaction [20] and measured fusion excitation function for this reaction (small open circles) [21]. Theoretical predictions [17] (solid lines) represent the product of the sticking cross section given by Eq. (4) (thick solid line) and survival probability calculated with the Monte Carlo method. Figure taken from [17].

effects, pairing and nuclear deformations (see Ref. [3], Appendix B). With one exception, mentioned in Sec. 12, we have been disregarding the shell correction at the fission saddle point, relying on the approximate validity of the topographic theorem (see next Section). In the case of the neutron emission saddle we use for the shell correction the expression due to Ignatyuk et al. [22]. We have found an algebraic approximation accurate to 1% for N_n , an integral over the Ignatyuk

level density. This leads to an entirely algebraic formula for N_n/N_f .

12 The topographic theorem

This theorem explains why even large shell effect fluctuations that may be present in the nuclear deformation energy landscape, are expected to have only a small effect on the energy of a saddle point present in such a landscape. Following the conventional treatment of nuclear deformation energies, imagine the deformation energy landscape to consist of a smooth macroscopic (liquid drop like) background in the form of a saddle, modified by shell correction oscillations of relatively short range that produce local bumps and hollows in the overall saddle-like landscape. In seeking the most economical way of crossing from one low region of the pockmarked saddle to the other, a hiker will certainly avoid going over a bump: he can do better by going around it. But it will also do him little good to go into one of the localized hollows, since he will have to climb out of it again to get anywhere. So in his search for the best way to cross the pock marked saddle he will avoid bumps and ignore hollows. It follows that the lowest energy that he will eventually encounter in his crossing will not be very different from what it would have been if the bumps and hollows had not been there in the first place! This means that shell corrections to macroscopic saddle point energies will be small even if the shell oscillations themselves are large. This expectation is confirmed directly by plotting some 120 measured saddle point masses, available in the range $Z = 71$ to $Z = 100$, as a function of the neutron and proton numbers and verifying that the deviations from smoothness are on the average only about 1 MeV [23], see Fig. 9.

One implication of the topographic theorem is that for heavy nuclei, where the macroscopic fission barrier is about to vanish, and the mass of the macroscopic saddle point is thus close to the macroscopic mass of the sphere, the mass of the fission saddle point even in the presence of shell effects will be close to the mass of the macroscopic sphere. This provides a remarkably simple first estimate of the fission saddle point mass required for calculating the number of channels N_f as well as for estimating the barrier height H entering the diffusion equation (2). However, it is for such heavy nuclei, especially those beyond the point where the macroscopic barrier has vanished,

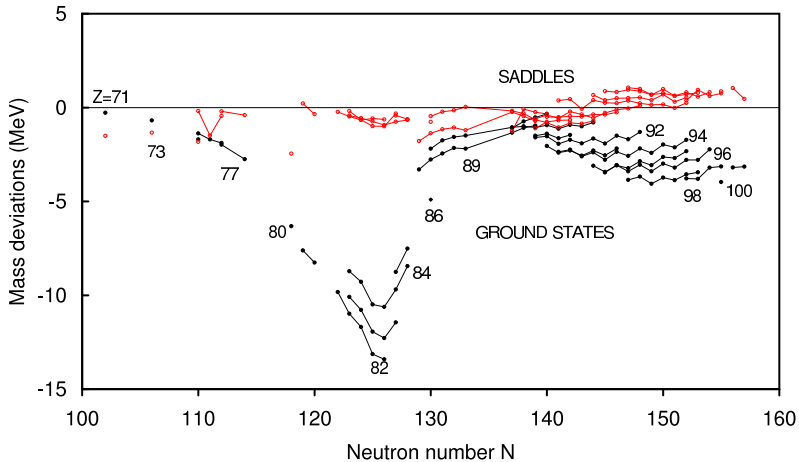


Figure 9: The black circles represent ground-state shell corrections (deviations of measured ground state masses from masses of the spherical configuration calculated using the Thomas-Fermi theory [24, 25]). Isotopes are connected by lines and the labels help to identify the atomic numbers. The red (open) circles represent shell corrections to macroscopic saddle point energies (deviations of measured saddle masses from calculated Thomas-Fermi saddle masses [26]). Figure taken from [23].

that a systematic deviation from the above elementary estimate may appear for nuclei stabilized by a shell effect. In particular, if a macroscopically unstable nucleus is stabilized by a shell effect in a prolate equilibrium shape, its saddle point will be a configuration with a deformation exceeding the equilibrium deformation by an amount at least sufficient to make the shell correction vanish. The resulting deformation may be quite substantial. Even if, in the spirit of the topographic theorem, we disregard the shell corrections beyond the point where the shell correction vanished, the macroscopic energy at the location of the saddle thus estimated will be below the energy of the unstable macroscopic sphere. This energy difference will grow with increasing fissility of the nucleus, and it may eventually attain a non-negligible magnitude. On the other hand, for very heavy nuclei stabilized by a shell effect in the spherical, rather than in a deformed

configuration, the saddle will also be close to the sphere and the above correction will be much smaller. We have developed a simple prescription for estimating these corrections to the basic version of the topographic theorem (see Ref. [3], Appendix B.2).

13 The anatomy of a fusion excitation function

By putting together the above estimates of “Stick”, “Diffuse” and “Survive”, each a function of the center of mass energy E , we can calculate the excitation function for a one-neutron-out cold fusion reaction using Eq. (3).

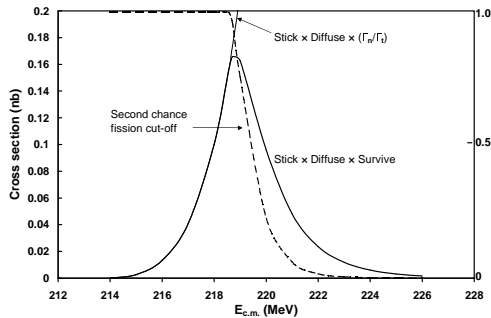


Figure 10: The anatomy of a one-neutron-out excitation function for the reaction $^{58}\text{Fe} + ^{208}\text{Pb} \rightarrow ^{265}\text{108} + \text{n}$ (see text). Figure taken from [3].

The qualitative appearance of this excitation function follows on general grounds, as illustrated in Fig. 10. It begins its exponential-like increase at the threshold energy for neutron emission, below which N_n is zero, and above which the factors “Stick”, “Diffuse” and N_n/N_f all increase rapidly. This increase is, however, turned into a decrease,

usually within less than an MeV, by the even more rapidly decreasing exponential cut-off given by Eq. (5). There follow two interesting predictions. First, the anticipated shape of the excitation function is not at all like a Gaussian, but more like two exponentials, one increasing one decreasing, with a slightly rounded-off intersection. The Gaussian-like appearance of most measured cold fusion excitation functions is due to the dispersion of the bombarding energy in a typical target. Second, the peak of the excitation function, close to the intersection region, is determined almost uniquely by the threshold E_{th} for second chance fission or second neutron emission, whichever is lower. It is readily verified that this leads to the following “optimum energy rule”: (Ref. [3], Sec. V)

The optimum center-of-mass bombarding energy in a one-neutron-out heavy ion reaction designed to make a mass A compound nucleus, exceeds by an amount of the order of an MeV either the mass of the fission saddle point of the residual nucleus $(A - 1)$ plus the mass of a neutron, or the mass of the residual nucleus $(A - 2)$ plus the mass of two neutrons, in both cases reduced by the sum of the masses of target and projectile.

In Figs. 11 and 12 we show two examples of measured excitation functions for synthesis of superheavy elements of $Z = 108$ and 104 in two cold fusion $^{208}\text{Pb}(^{58}\text{Fe},1n)^{265}\text{Hs}$ and $^{208}\text{Pb}(^{50}\text{Ti},1n)^{257}\text{Rf}$ reactions, respectively. These excitation functions are compared with our theoretical excitation functions. Within the accuracy of ± 1 MeV the maxima of the measured distributions agree with our “optimum energy rule”.

Note that neither the entrance channel (sticking) barrier nor the Coulomb or Bass’ reaction barrier, are relevant to the location of the excitation function maximum.

14 The role of the entrance channel barrier

The last statement needs to be qualified. Even though it is true for most cold fusion reactions under study, the entrance channel barrier does influence the *shape* of the excitation function and, in extreme situations, could influence even its location. In a typical cold fusion reaction the threshold E_{th} turns out to be below B_0 by up to a few

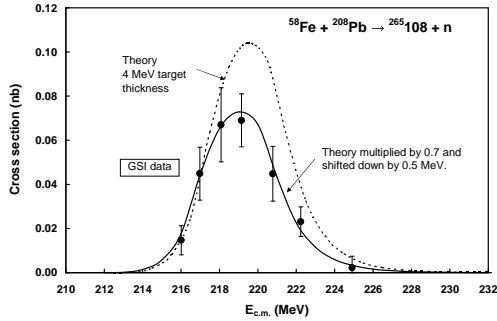


Figure 11: Comparison of the theoretical excitation function for the $^{58}\text{Fe} + ^{208}\text{Pb} \rightarrow ^{265}\text{Hs} + n$ reaction with measurements. The dotted curve is the theoretical excitation function convoluted with a (rectangular) spread in center of mass beam energy of 4 MeV caused by the finite target thickness. The solid curve results from multiplying the dotted curve by 0.7, and shifting it down by 0.5 MeV. These numbers are a measure of the discrepancy between theory and experiment. Note that the predicted width of the excitation function agrees with measurement. Figure taken from [3].

MeV, in the region where the sticking cross section is decreasing at an accelerating rate, but not yet where the limiting trend of a Gaussian tail has asserted itself. For such values of $B_0 - E_{th}$ the cut-off due to Eq. (5) is able to turn down the heretofore rising cross section within no more than an MeV. With increasing $B_0 - E_{th}$, however, the competition between the rising cross section and the cut-off becomes more evenly balanced. As a result, the energy of the turnover point increases somewhat and the high energy tail of the cross section becomes longer. This leads to a noticeable asymmetry (skewness) of the excitation function. The tail is being “pulled out” by the increasing distance between the mean barrier B_0 and the threshold E_{th} . Eventually, with a sufficiently large “pulling power” $B_0 - E_{th}$, one enters the

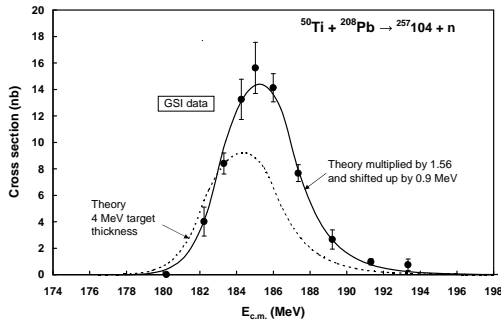


Figure 12: This is like Fig. 11, but for the reaction $^{50}\text{Ti} + ^{208}\text{Pb} \rightarrow ^{257}\text{Rf} + n$. Figure taken from [3].

region where the Gaussian increase with energy of the sticking cross section overpowers the exponential decrease due to the cut-off, as must always happen eventually in a competition between a Gaussian and an exponential. The turn-over point in the excitation function gets “unstuck” from the vicinity of E_{th} and is forced to follow B_0 at a distance that is not allowed to become too large.

These are the theoretical predictions that follow from the balancing of an exponential cut-off and a sticking cross section that tends to a Gaussian for low energies. Recent measurements at the Berkeley Gas filled Separator using very thin targets appear to provide evidence in line with the above expectations.

15 Theory and measurements

In the above we gave a descriptive outline of the physics that goes into the “Fusion by Diffusion” approach. A particular implementation of this approach is described in [3]. A survey is provided there of the relation of theory to measurements on 12 excitation functions

producing elements with $Z = 102$ to $Z = 112$ and the details of the separate factors “Stick”, “Diffuse” and “Survive” are discussed. In that reference one adjustable parameter was introduced, the critical injection distance s between the nuclear surfaces at which the neck zip is assumed to take place. Its value turned out to be $s = 1.6$ fm. The cross sections calculated within this particular implementation of the fusion by diffusion model are shown in Fig.1, while predictions regarding the optimum bombarding energies for 1n reaction are illustrated in Figs.11 and 12. It is seen from these comparisons that at least for the class of cold fusion reactions the production cross sections are very well reproduced by the theory, and moreover the optimum bombarding energies, the key factor in planning long search experiments, can be quite accurately predicted.

Acknowledgements

We have benefited from discussions and correspondence with Jan Blocki, Sigurd Hofmann, Kosuke Morita, Yuri Oganessian, Zygmunt Patyk and Adam Sobczewski. We would also like to thank members of the Berkeley Heavy Element Nuclear and Radiochemistry Group for discussions and for sharing recent experimental results. This work was supported in part by the D.O.E. under contract No. DE-AC03-76SF00098 (LBNL) and by the Polish Ministry of Science and Higher Education under Grant MNiSW No. 1 P03B 090 29.

References

- [1] S. Hofmann, Rep. Prog. Phys. **61**, 639 (1998).
- [2] Y. Oganessian, J. Phys. G: Nucl. Part. Phys. **34**, R165-R242 (2007).
- [3] W. J. Świątecki, K. Siwek-Wilczyńska and J. Wilczyński, Phys. Rev. C **71**, 014602 (2005).
- [4] W. J. Świątecki, K. Siwek-Wilczyńska and J. Wilczyński, Acta Phys. Pol. **B34**, 2049 (2003).
- [5] W. J. Świątecki, K. Siwek-Wilczyńska and J. Wilczyński, J. Mod. Phys. **E13**, 261 (2004).

- [6] K. Morita et al., *J. Phys. Soc. Japan* **73**, 1738 (2004).
- [7] J. P. Blocki, H. Feldmeier and W. J. Swiatecki, *Nucl. Phys.* **A459**, 145 (1986).
- [8] H. Riske, *The Fokker-Planck Equation*, (Springer-Verlag, Berlin, 1989).
- [9] J. Blocki and W. J. Swiatecki, Lawrence Berkeley Laboratory preprint LBL-12811, May 1982.
- [10] R. Bass, *Nucl. Phys.* **A231**, 45 (1974).
- [11] K. Siwek-Wilczyńska and J. Wilczyński, *Phys. Rev. C* **69**, 024611 (2004).
- [12] J.R. Leigh, M. Dasgupta, D.J. Hinde, J.C. Mein, C.R. Morton, R.C. Lemmon, J.P. Lestone, J.O. Newton, H. Timmers, J.X. Wei, and N. Rowley, *Phys. Rev. C* **52**, 3151 (1995).
- [13] C.R. Morton, A.C. Beriman, M. Dasgupta, D.J. Hinde, J.O. Newton, K. Hagino, and I.J. Thompson, *Phys. Rev. C* **60**, 044608 (1999).
- [14] M. Trotta, A.M. Stefanini, L. Corradi, A. Gadea, F. Scarlassara, S. Beghini, and G. Montagnoli, *Phys. Rev. C* **65**, 011601(R) (2001).
- [15] A.M. Stefanini, D. Ackermann, L. Corradi, D.R. Napoli, C. Petrache, P. Spolaore, P. Bednarczyk, H.Q. Zhang, S. Beghini, G. Montagnoli, L. Mueller, F. Scarlassara, G.F. Segato, F. Soramel, and N. Rowley, *Phys. Rev. Lett.* **74**, 864 (1995).
- [16] A.M. Stefanini, D. Ackermann, L. Corradi, J.H. He, G. Montagnoli, S. Beghini, F. Scarlassara, and G.F. Sagato, *Phys. Rev. C* **52**, R1727 (1995).
- [17] K. Siwek-Wilczyńska, I. Skwira and J. Wilczyński, *Phys. Rev. C* **72**, 034605 (2005).
- [18] R. N. Sagaidak, V. I. Chepigin, A. P. Kabachenko, A. Yu. Lavrentev, O. N. Malyshev, Yu. Ts. Oganessian, A. G. Popeko,

- J. Roháč, A. V. Yeremin, S. Hofmann, F. P. Hessberger, V. Ni-
nov, and C. Stodel, in *Proceedings of VI International School-
Seminar "Heavy Ion Physics,"* Dubna, 1997, edited by Yu. Ts.
Oganessian and R. Kalpakchieva (World Scientific, Singapore,
1998), p. 323.
- [19] C. R. Morton, A. C. Berriman, M. Dasgupta, D. J. Hinde, J.
O. Newton, K. Hagino, and I. J. Thompson, *Phys. Rev. C* **60**,
044608 (1999).
- [20] T. Sikkeland, J. Maly, and D.F. Lebeck, *Phys. Rev.* **169**, 1000
(1968).
- [21] T. Murakami, C. C. Sahm, R. Vandenbosch, D. D. Leach, A.
Ray, and M. J. Murphy, *Phys. Rev. C* **34**, 1353 (1986).
- [22] A. V. Ignatyuk, G. N. Smirenkin and A. S. Tishin, *Yad. Fiz.* **21**,
485 (1975) [*Sov. J. Nucl. Phys.* **21**, 255 (1975)].
- [23] W. J. Świątecki, K. Siwek-Wilczyńska and J. Wilczyński, *Acta*
Phys. Pol. **B38**, 1565 (2007).
- [24] W.D. Myers, W.J. Swiatecki, *Nucl. Phys.* **A601**, 141 (1996).
- [25] W.D. Myers, W.J. Swiatecki, *Table of Nuclear Masses ac-
cording to the 1994 Thomas-Fermi Model*, Lawrence Berkeley
Laboratory report LBL-36803, December 1994. Accessible on
<http://ie.lbl.gov/txt/ms.txt>.
- [26] W.D. Myers, W.J. Swiatecki, *Phys. Rev.* **C60**, 014606 (1999).